Experimental analysis of the station keeping response of a double-barge float-over system with an elastically scaled physical model

Daniele Dessi, Edoardo Faiella, Francesco Saltari
Marine Technology Research Center, National Research Council
Rome, Italy
Corrado Pigna, Cristiano Celli, Thiago Miliante[1], Enrico Di Paolo
TechnipFMC Rome Operating Center
Rome, Italy

ABSTRACT

In this paper, an experimental investigation of the global response to waves relative to a newly developed float-over concept by TechnipFMC Rome Operating Center for transportation, installation and decommissioning of the off-shore platform topside is presented. A flexible scaled model of the float-over system was tested in the wave basin to determine the range of the sea-state conditions for which the response of the catamaran float-over is acceptable for mating operations. The present analysis is part of a more extensive experimental campaign which has involved also the use of a scaled rigid physical model (Dessi et al., 2016) and numerical simulations for which the collected data provide also a validation database.

KEY WORDS: Catamaran float-over; topside installation; asymmetric barge; flexible physical model; hydroelasticity; station keeping tests; mooring system.

INTRODUCTION

The topside deployment has been typically carried out using lifting cranes equipping special vessels. To find reliable and affordable alternatives, floating systems based on the use of single or twin barge arrangements have been also exploited for transportation, installation and decommissioning of the off-shore platform topside for jacket structures (see, e.g., , Kurian et al., 2012). An interesting market segment for this kind of operation includes topsides whose weight is in the range of 1000-3000 tons, for which is uncommon using float-over systems especially in a catamaran arrangement. For this reason, TechnipFMC Rome Operating Centre (ROC) has been developing a reliable and innovative catamaran float-over (CFO) concept based on the use of not-identical barges and properly re-designing the supporting structure, increasing the usability of this concept so as to be a valid alternative in areas characterized by lack of lifting capabilities. The transportation and installation procedures require preliminary analysis of the global response of the considered float-over configuration to the waves due to the strict met-ocean margins for safe operations. For a single barge, Duquesnay et al. (2013) investigated the approach to the slot under the action exerted by the tug towing lines, the mooring lines and the cross lines. Luo et al. (2013) considered the alternative float-over system based on use of a catamaran configuration highlighting the advantages with respect to the single barge. Beside the engineering interest in developing such system, the catamaran float-over is a challenging fluid-structure interaction problem. Globally the catamaran float-over appears as a floating system with an elastic link between the barges. The flexibility of the topside allows the possibility that one barge may move with respect to the other under proper wave excitation, determining a two-way coupling between the fluid and the structure.
Therefore, a detailed experimental investigation of the response of the catamaran float-over (CFO) system has been carried out at CNR-INSEAN towing-tank basin with a flexible connection between the not-identical barges. Following the first experimental campaign with the 'rigid' model (Dessi et al., 2016), more focused on the transportation phase, the flexible physical model was tested with waves having different relative directions. To keep the catamaran position and heading stable under the wave excitation, a mooring system made of horizontal lines was used. Several physical model data were acquired during the tests: the wave elevation, the 6-dof motion of each barge, and the bending moment at the topside connections with the barges. From these measurements, the relative motion between the barges could be evaluated, pointing to combinations of wave lengths and headings enhancing these coupled relative rotations. The large amount of collected data finally constitutes a database for the validation of seakeeping codes under development aimed to get a full-picture of the system response under a wider set of vessel speeds and wave headings.

OBJECTIVES OF THE INVESTIGATION

CFO layout

The catamaran float-over system is based on twin barges which carry

[1] Actually working at TechnipFMC Paris Operating Center.

on the topside to be installed on the jacket structure. The topside plays the role of a catamaran deck, keeping the two barges in the same reciprocal position under the wave excitation. As outlined in the introduction, TechnipFMC ROC has introduced the use of two similar, but not identical hulls in order to increase the adaptability of the concept accordingly to the barge availability on the market. The topside is actually connected to the barges through a supporting structure, specially designed to firmly sustain the topside weight, and requires proper ballasting of the barges to balance the residual roll and pitch moments in still water. The heel and trim of the barges are set to be zero so that the draft is uniform. The waterline level is rather high to guarantee the maximum stability and will be varied during the mating operations. The data relative to the tested configuration are reported in non-dimensional form in Table 1.

Table 1. Main geometrical and mass parameters of the catamaran

Parameter	Symbol	Value
Average barge length	L_r	96 m
Overall displacement	M_{CFO}	19552 tons
Model scale	λ	40
CFO breadth	B / L_r	0.885
Gap between barges	b / L_r	0.25
Draft	d / L_r	0.0412
CoG coordinates with respect to CFO ref. sys.	x_{CG}/L_r, y_{CG}/L_r, z_{CG}/L_r	-0.002, 0.03, -0.001

Aim of the investigation

The analysis of the transportation phase has been carried out in another paper (jointly presented at this conference). Here the focus is on the elastic response of the CFO system floating without speed. This experimental campaign required a dedicated set-up to deal with (*i*) the analysis of the system response to waves, highlighting the possibility of relative motion between the barges, (*ii*) the evaluation of the loads acting on the flexible topside and (*iii*) the data collection for hydro-elastic code validation. For all these reasons, an elastically scaled catamaran was designed and tested.

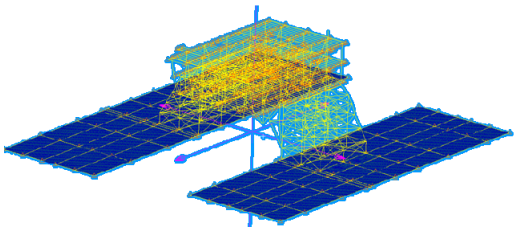

Fig. 1. Finite element model of the float-over system

HYDROELASTIC SCALING AND MODEL DESIGN

Reference finite element model

From a general point of view, the hydroelastic scaling and design of a physical flexible model requires preliminary the identification of the elastic features more involved in the response to the wave excitation. Therefore, a finite element (FE) model was specially prepared for the calculation of the vibration modes upon which the correspondence between the reference structure and the simplified scaled model has been set. At this level, the barges were assumed to be 'rigid' and their mass distribution was equivalently represented with shell elements (Fig. 1). The barge model includes also the water added mass using acoustical elements on the bottom barge side. The first six 'wet' vibration modes (excluding the CFO global rigid modes), sorted in ascending order with respect to the frequency, are reported in Figs. 2~4.

The elastic vibration modes can be roughly subdivided into several groups. Modes #1, #2, #3 are named 'Spring-like Modes,' because the connecting structure behaves like a torsional spring, and the barges appear to rotate with opposite angles. Modes #4 and #5 are called 'Balanced modes' instead, because the barges co-rotate this time, but the topside seems to be twisted along the same axis but in the opposite direction. Finally, from mode #6 on, more complicated modes involving evident distortion of the top-side or just local modes appear.

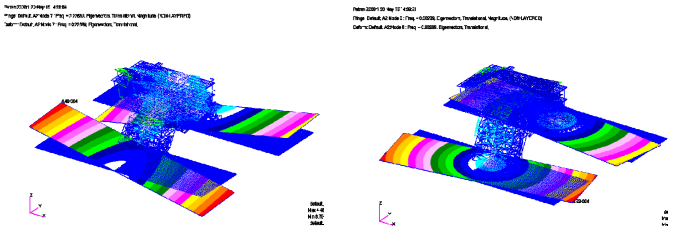

Fig. 2. #1 mode at 0.226 Hz (left, 3D view) and #2 elastic mode at 0.383 Hz (right, 3D view)

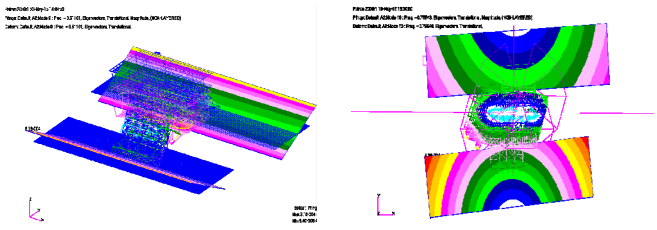

Fig. 3. #3 mode at 0.511 Hz (left, 3D view) and #4 elastic mode at 0.756 Hz (right, top view)

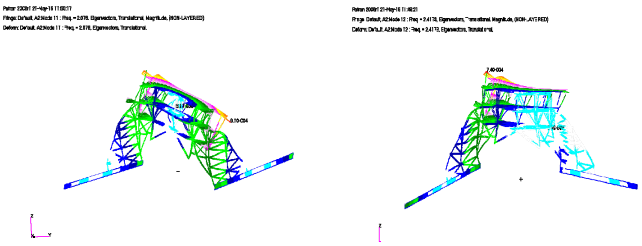

Fig. 4. #5 mode at 2.076 Hz (left, front view) and #6 elastic mode at 2.418 Hz (right, front view)

Scaling laws and reduced-order model

At model scale, applying the scaling relationship due to Froude, the scaling of velocity is obtained as:

$$\frac{v^{(S)}}{v^{(M)}} = \sqrt{\lambda} \qquad (1)$$

where λ is the ratio between the ship (S) and model (M) length, respectively. In this case, the average of the barge lengths is taken as

reference length. From this definition, it follows that the ratio of time scales is:

$$\frac{t^{(S)}}{t^{(M)}} = \sqrt{\lambda} \tag{2}$$

which in turn implies the following relationship between the full-scale and the model frequencies:

$$\frac{f^{(S)}}{f^{(M)}} = 1/\sqrt{\lambda} \tag{3}$$

The last relation ponts out that the vibration frequencies of the scaled model are increased with respect those of the full-scale structure. As a consequence of the above definitions, the other scaling relationships are set as follows:

Load and shear forces: $$\frac{F^{(S)}}{F^{(M)}} = \lambda^3 \tag{4}$$

Torques and bending moments: $$\frac{M^{(S)}}{M^{(M)}} = \lambda^4 \tag{5}$$

Bending stiffness: $$\frac{EI^{(S)}}{EI^{(M)}} = \lambda^5 \tag{6}$$

Shear rigidity: $$\frac{(GA^*)^{(S)}}{(GA^*)^{(M)}} = \lambda^3 \tag{7}$$

If the original or reference structure is collapsed into an equivalent model preserving the main topology features, the last two relations provide directly the sectional properties of the equivalent structure. This is typical for the structural scaling of the ship-beam (Dessi et al., 2008). In the present case, keeping the same topology also in the scaled model makes no sense from several points of view. Therefore, an equivalent structure has to be designed, and the equivalence can be established on a modal basis. The 'wet' frequency of the modes which one intends to assume as reference for the scaling is reported in Table 2. The set coincides with mode shapes shown in Figs. 2~4.

Table 2. Modal frequencies of the 3D reference structure (the frequencies are relative to their equivalent values at model-scale)

Mode	#1	#2	#3	#4	#5	#6
Reference mode frequency (Hz)	1.43	2.42	3.23	4.78	13.1	15.3

The relative importance of these modes for constructing a reduced-order model of the whole structure needs to be evaluated taking into account the sea excitation. A typical irregular sea following a Bretschneider spectrum with a significant wave period of T_s = 7.1*s* may excite the floating structure with the high-frequency side of its spectrum up to 0.25 *Hz*, or 1.58 *Hz* at model-scale. The wave length in the neighborhood of this frequency value is between the length of the transversal gap and half the barge length. Indeed, the excitation mechanism is mainly dominated by a spatial effect, and secondarily by the vicinity of the resonance. Thus mode #1 ('opposite pitch' or 'split' mode) and mode #3 ('opposite roll' mode) are likely to be excited by the wave system. Mode #2 is hardly spatially excited because the waves cannot produce opposite moments around the z-axis for the two barges separately. In any case, the resonance mechanisms might also enhance the response, but it is likely to happen only for mode #1. These observations lead to the conclusion that from a hydroelastic point of view we could limit to the 'Spring-like Modes' for the scaling process.

Reduced-order model

The design of the scaled elastic top-side considered many alternative configurations but keeping the number of structural elements as low as possible. The intermediate steps of the design process are not reported here for sake of conciseness. At the end we focused on a truss with four legs ("table-like" structure) plus some stiffeners, with an overall volume not far from that of the real topside, and connections to the barges close to the true position of the supporting structure basement. One of the key design features has been the choice of the rectangular hollow sections area of the columns and the openings on the column sides for tuning the overall torsional and bending stiffness. The adopted material for the connecting truss is aluminum. The truss design is shown schematically in Fig. 5, and in Fig. 6 the final structure is shown.

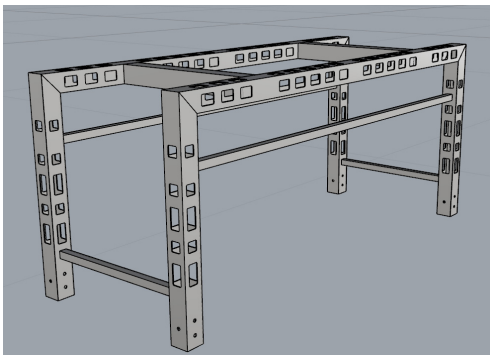

Fig. 5. 3D schematic view of the truss model

Fig. 6. Elastically scaled frame of the topside made of welded aluminum beams

The finite element analysis (FEA) of the structure led the design process. In Fig. 7 the global finite element model of the scaled flexible catamaran is shown. In Figs. 8~10 the scaled 'Spring-like Modes' shapes are shown, whereas in Table 3 the comparison between their frequencies and the reference frequencies is shown in terms of relative variation. Note that in Table 3 the modes are sorted not respect to their frequencies but accordingly to their correspondence with the true modes. In general, the correspondence of modal shapes between the two sets is fair. However, the general increase of frequencies (with only one exception) points out that the scaled structure is stiffer than the reference one. This result is also confirmed by the computation of the stiffness matrix between the two barges that was carried out in MSC-NASTRAN using super-elements. This stiffness matrix is a symmetric square matrix, being 12x12 because of the barge asymmetry. The norms of the full-scale and the physical model stiffness matrices, reported at the same scale, are 1.15e+11 and 3.01e+11, respectively.

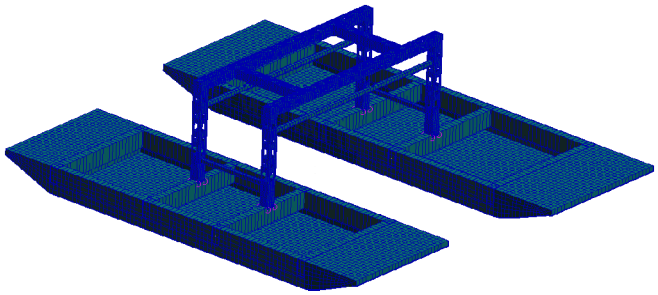

Fig. 7. Finite element model of the scaled physical model

Table 3. Modal frequencies of the FE model of the elastically scaled catamaran (errors are relative to the reference structure, values at model scale)

Mode	#1	#2	#3	#4	#5	#6
Modal frequency (Hz)	1.49	4.2	3.93	6.20	7.83	20.7
% error	+4.2	+73	+22	+29	-40	+36

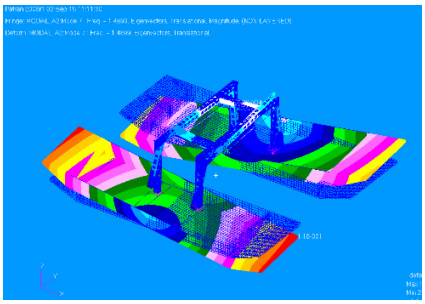

Fig. 8. #1 elastic mode at 1.49 Hz (Opposite pitch or split mode)

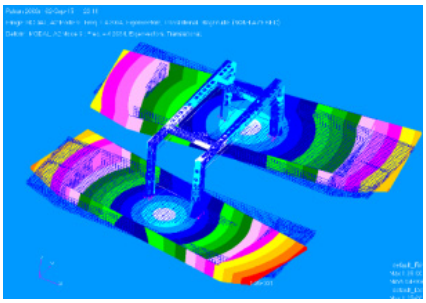

Fig. 9. #2 elastic mode at 4.2 Hz (Opposite-yaw mode)

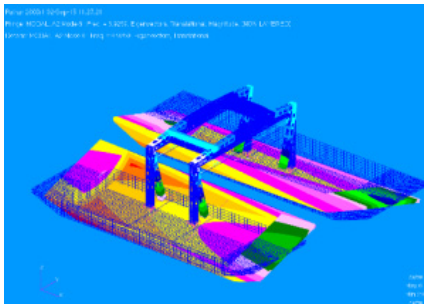

Fig. 10. #3 elastic mode at 3.93 Hz (Opposite-roll mode)

EXPERIMENTAL SET-UP

Model construction

The flexible scaled model used the same barges of the rigid model (Dessi et al., 2017) with a different layout of the inner metallic frame to provide support to the topside. To link the topside to the transverse bars was necessary to build four mechanical joints which can slide along each bar to set the correct position of the legs. They were obtained by machining aluminum blocks to provide geometrical accuracy and stiff connections between the parts. Ballasting of the barges required particular care in this case. In the case of the rigid catamaran, the CoG has to be set in the right position for achieving the desired heel and trim of the whole vessel. When the barges are connected elastically to each other, each barge has to be ballasted separately in order to find the desired equilibrium between the buoyancy force, the weight and the force exchanged with the twin hull. The final arrangement is shown in Fig. 11.

Mooring system

The mooring system was specifically designed for the analysis of the station keeping behavior, a condition occurring during the final mating operations. From an experimental point of view, the goal was keeping the physical model in a prescribed position and orientation with respect to the carriage in the wave basin, without any link to a real situation. Therefore, a horizontal layout of the mooring lines was preferred because with this arrangement seakeeping predictions at zero speed can be compared with experimental data in the dofs not affected by the presence of the mooring lines, i.e., heave, roll and pitch. The interference of the mooring system with the floating body motion was deeply investigated in one case by comparing the response of the “free” model with that exhibited by the constrained model. During the station keeping tests, the model appears to be ‘gently’ constrained in its position: this was obtained by fine-tuning of the line tension and by using a small piece of elastic string in the final connection to the model. The other end of the mooring line was attached to a hook located at the basin walls, near the waterline. It is worth to underline that the mooring line layout had to be modified every time the test heading was changed involving cumbersome tuning of the cable tension to achieve the desired yaw angle.

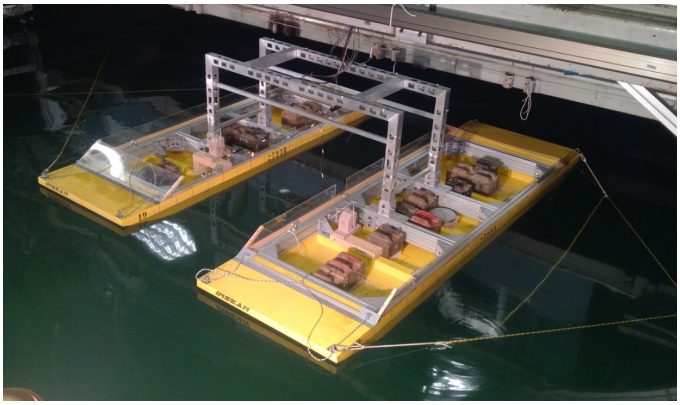

Fig. 11. Scaled flexible model in the towing tank

Sensor Equipment

The absolute wave height was measured in two positions with a finger probe which continuously follows the water surface thanks to a feedback signal; one was set upstream and the other was placed alongside the catamaran on-board the carriage. The rigid-body motion, consisting of 3 translations and 3 rotations relative to each barge was obtained with an optical system (Krypton). The Krypton cameras recorded independently the positions of two distinct targets, one on the small barge and the other on the big barge. These targets carry on flashing infrared leds actually identified by the optical system. Sixteen strain gages were placed at the base of the four columns, two on each inner face of the rectangular hollow beams, as shown in Fig. 12. No measurement of the mooring line tension was taken for this system does not reproduce any real arrangement. The acquisition system was the DEWE-soft Dewe-43 multi-channel DAQ system at a sampling rate of 100Hz.

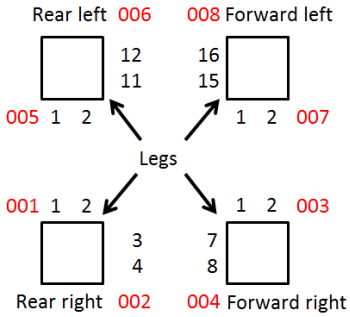

Fig. 12. Strain-gage layout on the truss legs (2-digit numbers = strain gage, 3-digit numbers = measurement point based on strain-gage couple)

EXPERIMENTAL RESULTS

Definitions

In the following, the experimental data relative to the elastic CFO are presented. First, it is worth defining the response amplitude operators (RAO) for the various dofs. In the case of regular waves they are defined as:

$$\text{Heave } RAO = \frac{\bar{\zeta}_A}{\bar{h}_A}, \quad \text{Roll } RAO = \frac{\bar{\phi}_A}{k_w \bar{h}_A}, \quad \text{Pitch } RAO = \frac{\bar{\vartheta}_A}{k_w \bar{h}_A} \tag{8}$$

where $\bar{\zeta}_A, \bar{\phi}_A, \bar{\vartheta}_A$ indicate the mean amplitude (average over the peak values) of heave, roll and pitch, respectively, $\bar{h}_A$ is the regular wave amplitude and $k_w = 2\pi/\lambda_w$ is the wave number, with λ_w the wave length. The RAO points are plotted with respect to the dimensional wave frequency at full scale. In a similar way the RAOs are also calculated with stochastic sea input, according to the following definitions:

$$\text{Heave } RAO = \sqrt{\frac{\zeta_{PSD}(f)}{h_{PSD}(f)}}, \quad \text{Roll } RAO = \frac{1}{k_w(f)}\sqrt{\frac{\phi_{PSD}(f)}{h_{PSD}(f)}}, \quad \text{Pitch } RAO = \frac{1}{k_w(f)}\sqrt{\frac{\vartheta_{PSD}(f)}{h_{PSD}(f)}} \tag{9}$$

where the power spectral density (PSD) is calculated with the Welch method that uses the periodogram technique applied to eight intervals with 50% overlap.

General features of the catamaran global motion

The station keeping response of the CFO is investigated for different relative headings with respect to the wave direction, both with regular and irregular seas, the latter following a Bretschenider spectrum. Different wave amplitudes and periods were spanned to have an estimation of the RAOs in all the frequency range of interest along with an indication of possible nonlinear features.

In the following Figs. 13~15 a global picture of the response in regular waves with respect to the full-scale frequency for different headings is given. In Fig. 14 the RAO plot shows that the amplitude of heave motion depends weakly on the wave heading. This probably is related to the similar longitudinal and transversal overall lengths of the catamaran (see Table 1). Response in head waves is slightly larger than in beam seas, whereas in oblique seas no much difference is present. In the case of roll (Fig. 15) and pitch (Fig. 16) motion amplitude depends on the wave heading to a greater extent. Beside the limit cases, with pitch and roll amplitudes close to zero in beam and head seas, respectively, it is worth noting that the pitch response in oblique seas is not far from the response in head waves. The same observation does not apply to roll. If one compares the roll and pitch RAOs in their most favorable wave direction, there is in both cases a mild resonance peak (this depends also on the adopted RAO definition), but it seems to occur at a lower frequency in the case of pitch. In general, it is acceptable that the roll response is more excited at shorter wave lengths than pitch.

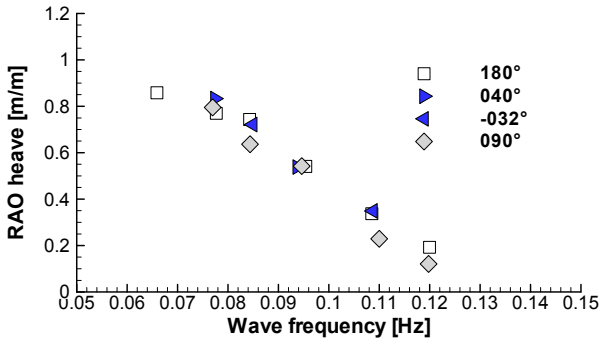

Fig. 13. Heave RAO in regular waves for different headings

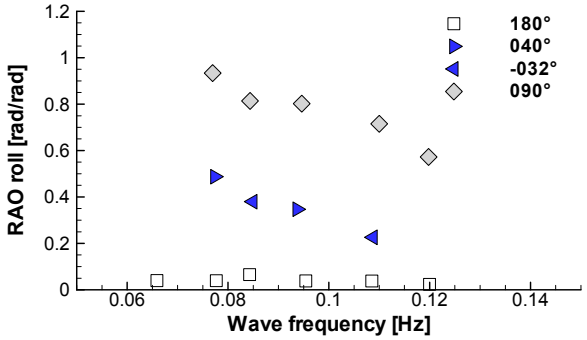

Fig. 14. Roll RAO in regular waves for different headings

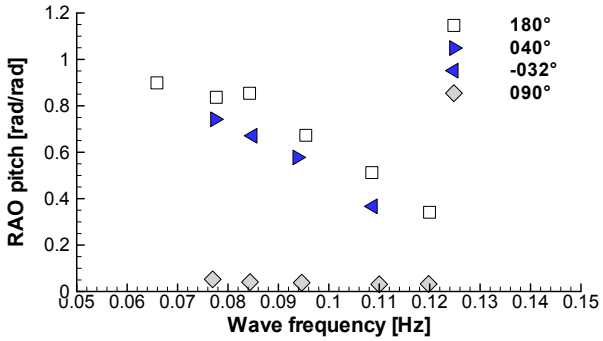

Fig. 15. Pitch RAO in regular waves for different headings

In (Dessi et al., 2017), jointly presented at this conference, the seakeeping behavior of the catamaran was considered. Comparing the data relative to the rigid and elastic topside configuration, no appreciable difference between the RAOs at the CoG due to the topside elasticity was highlighted. The spring constraint between the two barges allows relative motion, but with oscillations having opposite sign which keep the global CoG almost in the same position. Nonetheless, it cannot be excluded that the relative motion between the barges may gather and then dissipate mechanical energy from the waves, then reducing the amount of energy that is converted into global motions. It is just a matter of small quantities that will require further investigation or dedicated experiments.

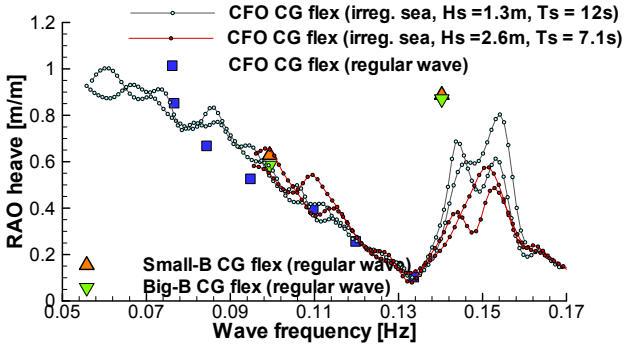

Fig. 16 Heave RAO in head waves

Analysis of barge relative motions

The FE analysis of the topside has highlighted that its deformation may be significant under the wave loads, and its order of magnitude is comparatively larger than those of the barges. Therefore, as first approximation, to interpret its global action it has been reasonable to assume that the topside plays as an equivalent spring system connecting the rigid barges. In the analysis presented in the following both the global CoG motion and the distinct responses of the barge CoG are analyzed in head waves (180°), oblique seas (around 225°) and beam seas (270°).

Regarding only the response of the catamaran CoG, in all the plots there is no much difference between irregular sea excitation and regular waves. In some cases, close to resonances, some differences may be present but no clear indications are available at this level. When the motion of each barge is considered, some attention has to be paid to the meaning of the involved quantities. Heave RAO in head waves is represented in Fig. 16 including the separate analysis of the barge motions which was obtained from different regular wave tests. For this reason, the colored triangles, one for the small and one for the big barge, refer to a wave frequency that may be slightly different from that relative to the CFO CoG, marked with a blue square. The heave oscillations of each barge are phased in head waves and the catamaran RAO is close to those relative to the barges. As expected, no significant differences are present considering that the two measurements refer to the same physical model but tested in two different experimental campaigns. Similar concepts apply also to Figs. 17~18. Fig. 19 and Fig. 22 relative to oblique sea and beam seas, respectively, show also rather different heave motions for certain wave lengths. In a global frame of reference, disregarding the effect of the topside flexibility, the motion of the barge CoG can be expressed as a combination of the catamaran CoG and its rotation around this point, according to the following expression:

$$\mathbf{x}_B(t) = [\mathbf{R}(t)]\,\mathbf{x}_{B,rel} + \mathbf{x}_{CFO}(t) \tag{10}$$

where $\mathbf{x}_B$ and $\mathbf{x}_{CFO}$ are the coordinates of the barge and the catamaran CoGs with respect to an inertial frame of reference, respectively, $\mathbf{x}_{B,rel}$ is the coordinate of the barge CoG with respect to the mobile reference system of the catamaran, and $[\mathbf{R}(t)]$ is the corresponding rotation matrix. Thus, if pitch or roll have large amplitudes, as $\mathbf{x}_{B,rel}$ is opposite for the two barges, the barge motions are different from each other.

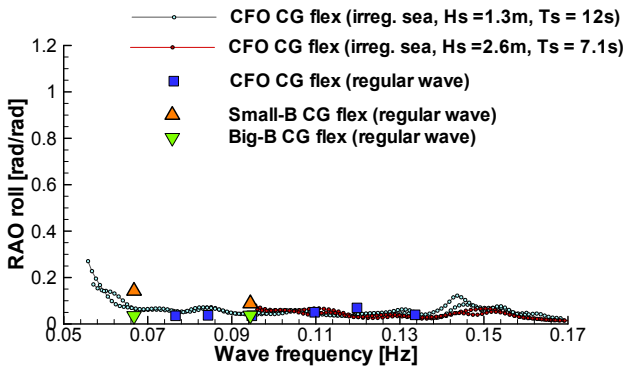

Fig. 17. Roll RAO in head waves

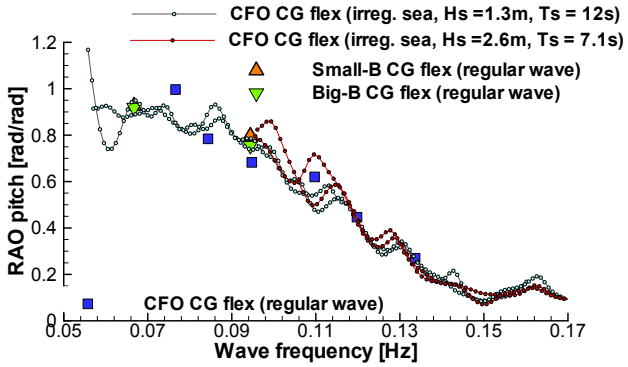

Fig. 18. Pitch RAO in head waves

Moreover, the amplitude of the CFO heave motion is not the average of the single-barge heave amplitudes, because it depends on the phasing between heave, pitch and roll of the catamaran.

The true features of the elastic motion can be better highlighted by examining the rotational dofs. In oblique seas (Figs. 20~21) the relative pitch motion is more evident than the roll motion and this depends on the higher stiffness of the roll elastic mode with respect to the pitch elastic mode. This stiffer behavior in the relative roll response is also present in beam seas as shown in Fig. 23. However, the values shown in the plot do not represent yet the amplitude of the relative roll motions because phase information between the two barge time-histories cannot be deduced. Figs. 24~25 show some results relative to the time-history of the difference between the rotational dofs of the two barges, or in other terms the relative barge rotations. The average amplitude of the signal is extracted and reported in the plots with respect to the incident wave frequency. The presence of a peak around 0.11 *Hz* is the most significant information. A similar analysis is presented in Fig. 25, but for oblique seas. Unfortunately, some conditions are missing to clearly deduce where peaks are. Something similar around or beyond 0.11 *Hz* is present, but a secondary peak also emerges between 0.08 and 0.09 *Hz*.

The effect of the different barge lengths can be highlighted by calculating the pitching bending moment from the strain-gage data. In Fig. 26 the amplitude of the (pitching) restoring bending moments are small with one exception relative to the regular wave test at the highest frequency (or shortest wave length). In this case, it is reasonable that some effect due to the different barge length may appear, determining a different hydrodynamic pitching moment that the topside structure has to balance. A similar result is also shown for oblique sea in Fig. 27 following a trend for the restoring moment close to the trend of relative pitch rotations shown in Fig. 25.

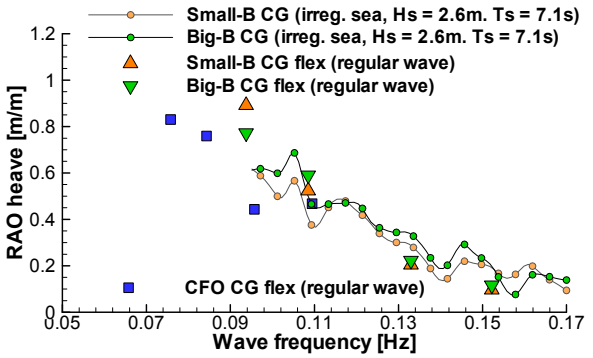

Fig. 19. Heave RAO in oblique seas

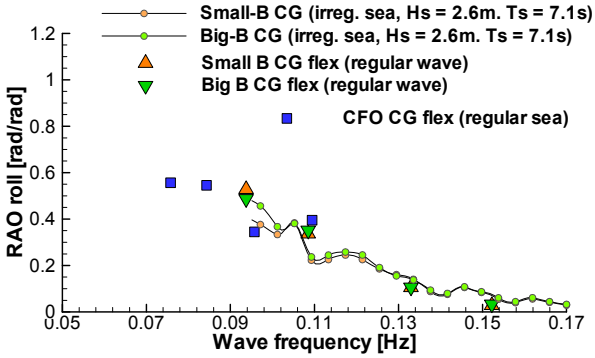

Fig. 20. Roll RAO in oblique seas

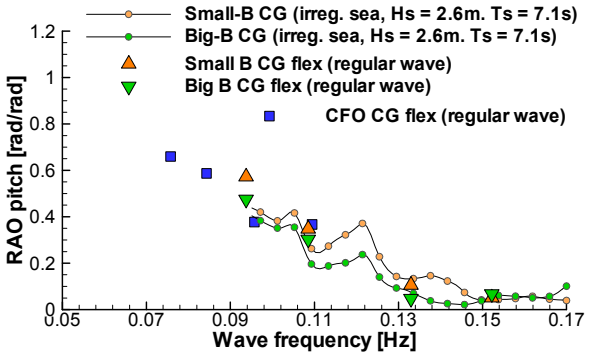

Fig. 21. Pitch RAO in oblique seas

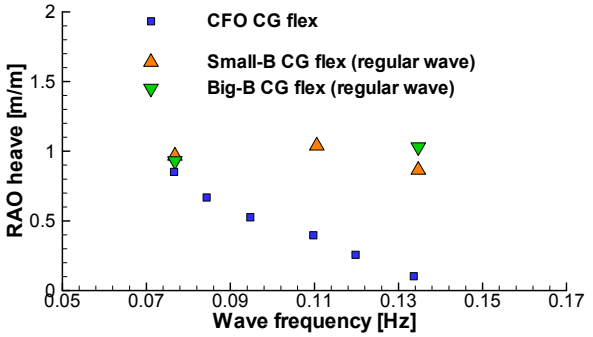

Fig. 22. Heave RAO in beam seas

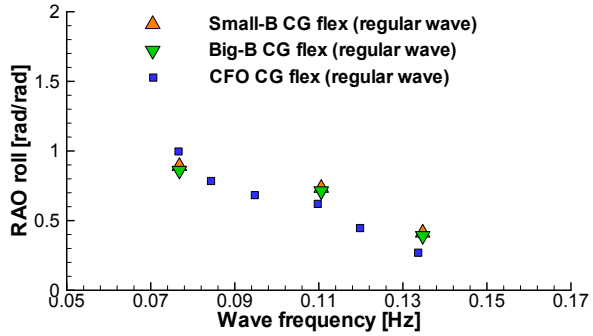

Fig. 23. Roll RAO in beam seas

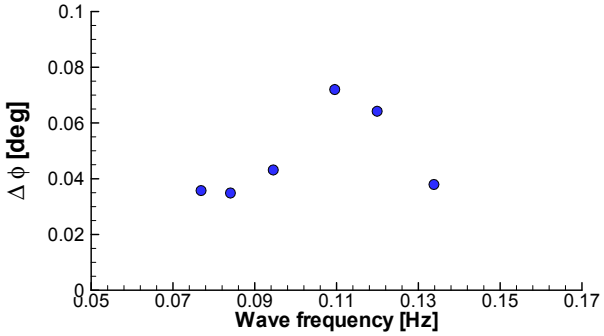

Fig. 24. Relative roll between the barges in beam seas

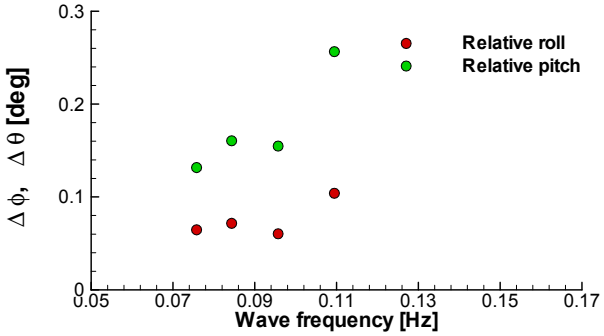

Fig. 25. Absolute relative roll and pitch between the barges in oblique sea

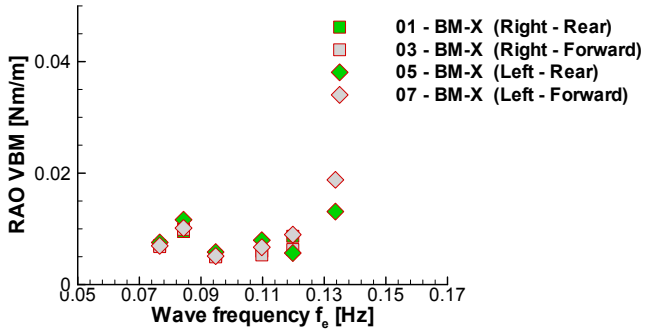

Fig. 26. Restoring (pitching) bending moment at the bottom of the vertical columns in head waves

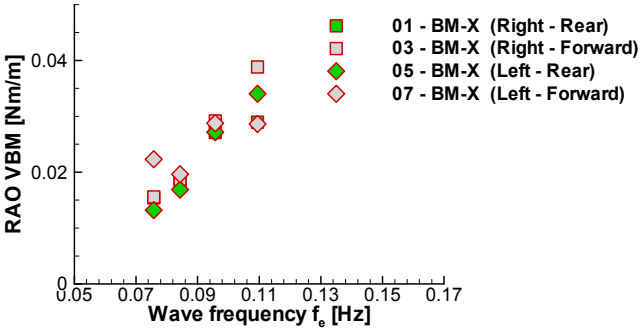

Fig. 27. Restoring (pitching) bending moment at the bottom of the vertical columns in oblique sea

CONCLUSIONS

The hydroelastic scaling of the essential modal properties of a real structure is a challenging problem under multiple technological and time constraints. The satisfactory correspondence between the full-scale and model-scale modal shapes and between the corresponding frequencies of the split mode (the most excited one) has allowed investigating also quantitatively the relative motion between the barges due to the flexible link provided by the topside. The prime effect of the flexibility is indeed on the relative pitch and roll motion, whereas its effect on the global catamaran motions appears negligible.

ACKNOWLEDGEMENTS

This work has been carried out under TechnipFMC Purchase Order ITENG000159. We wish also to thank Francesca Sindici for her fruitful support during the experimental campaign.

REFERENCES

C. Coppotelli, D. Dessi, R. Mariani, M. Rimondi (2008). "Output-only analysis for modal parameters estimation of an elastically scaled ship". Journal of Ship Research, Vol. 52(1), 45-56.

D. Dessi, E. Faiella, C. Pigna, C. Celli, T. Miliante, E. Di Paolo (2017). "Experimental analysis of topside transportation with a double-barge float-over system". Submitted for *The 27th International Ocean and Polar Engineering Conference*, San Francisco, CA, June 25-30.

P. E. Duquesnya, J. Baldwin and J. W. Rains (2013). "Docking and Undocking Considerations for Floatover Analyses and Operations". *Proc ASME 2013, 32nd International Conference on Ocean, O shore and Arctic Engineering*, OMAE2013-11340, Nantes, France, June 9-14.

V. J. Kurian, N. H. Baharuddin, A. M. Hashim and A. R. Magee (2012). "Dynamic Responses of Float-over Barge Subjected to Random Waves". *Proc 22nd International O shore and Polar Engineering Conference*, Rhodes, Greece, June 17-22.

M. Y. H. Luo, D. Edelson, J. Wan, J. Sun and S. Hassanaliaragh (2013). "Improvements in Heavy Topside Intsallation onto Spar Hull by Catamaran Floatover Method". *Proc ASME 2013, 32nd International Conference on Ocean, Offshore and Arctic engineering*, OMAE2013, Nantes, France, June 9-14.